Pergamon

Int. Comm. Heat Mass Transfer, Vol. 26, No. 6, pp. 781–790, 1999

0735-1933/99/$–see front matter

PII S0735-1933(99)00066-4

WALL EFFECTS ON THE RISE OF SINGLE GAS BUBBLES IN LIQUIDS

R. Krishna, M.I. Urseanu, J.M. van Baten and J. Ellenberger
Department of Chemical Engineering
University of Amsterdam
Nieuwe Achtergracht 166, 1018 WV Amsterdam
The Netherlands

(Communicated by E. Hahne and K. Spindler)

ABSTRACT

We report the results of an extensive experimental investigation on the velocity of rise of air bubbles in the size range d_b = 3 – 80 mm in water. Measurements were made in columns with inside diameters D_T = 0.01, 0.02, 0.03, 0.051, 0.1, 0.174 and 0.63 m. The column diameter was found to have a significant effect on the rise velocity of the bubbles. When the ratio of the bubble diameter to the column diameter, d_b/D_T, is smaller than 0.125 the influence of the column diameter on the rise velocity is negligible and the rise velocity is described quite accurately by the Mendelson equation. With increasing d_b/D_T there is a significant reduction of the rise velocity, i.e. there is a significant "wall effect". The wall effect for spherical cap bubbles rising in inviscid flow, obtained for bubble diameters larger than 0.017 m, is described adequately by the Collins relation. The wall effect for bubbles smaller than 0.017 m is described by an empirical relation suggested by Clift, Grace and Weber. © 1999 Elsevier Science Ltd

Introduction

In many branches of technology there is a need to estimate the rise velocity of gas bubbles in liquids. The rise velocity of bubbles can be affected to a significant extent by the dimensions of the containing vessel and a variety of empirical relations are available to quantify this effect [1,2,3]. Though there is a large variety of experimental data on rise velocity available in the literature for different bubble sizes and column diameters, it is difficult to compare the results of one set of authors with those of others because of: (1) differences in the physical properties of the liquids used in the various studies, (2) presence of impurities in the liquid phase, and (3) the fact that each study is often restricted to a narrow bubble size range in a given column diameter. In the present study we report the results of a comprehensive set of experiments on the bubble rise velocity for the bubble size range 3 – 80 mm in a variety of column diameters D_T = 0.01, 0.02, 0.03, 0.051, 0.1, 0.174 and 0.63 m. The objective of this study is to examine the accuracy of available literature correlations.

Experimental

The experiments were carried out in seven cylindrical columns with different inside diameters. Four of these columns, of 0.01, 0.02, 0.03 and 0.051 m inside diameters were made of glass. The remaining three columns, of 0.1, 0.174 and 0.63 m inside diameters, were made of polyacrylate sections. Figure 1 shows three typical experimental set-ups. In all the experiments the top of the column was operated at atmospheric pressure. Demineralized water (viscosity μ_L = 0.001 Pa s; density ρ_L = 998 kg/m^3; surface tension σ = 0.072 N/m) was used as liquid phase and air as gaseous phase. A set of experiments were also carried out with high viscous Tellus oil (μ_L = 0.075 Pa s; ρ_L = 862 kg/m^3; σ = 0.028 N/m) as the liquid phase. The experimental conditions are specified in Table 1.

For each experiment a single air bubble was injected at the bottom of the column using a standard medical syringe (syringes of different capacities were used in order to cover a wide range of bubble diameters). The 0.1, 0.174 and 0.63 m diameter columns were equipped with a ladle, which was mounted above the injection system, to allow bigger and more accurate gas volumes. To obtain the desired bubble volume the air was added into the ladle, by injecting air repeatedly with the small syringe. The bubble was released by inverting the ladle. With this system it was possible to obtain bubbles with the equivalent diameter in the range: 3 to 80 mm. The time elapsed for the single bubble to rise between predetermined markers was measured using a stopwatch. The distance between the two markers differed from column to column. In order to see the bubble passing the upper marker, a Sony colour video monitor was used. The Panasonic DSP colour CCD camera was focussed on the upper marker. The ambient light level was improved using a 1250 W halogen lamp.

Experimental Results

According to the criterion discussed in Clift et al. (1978) we may expect the bubble rise velocity to be independent of wall effects when the ratio of the bubble diameter to column diameter is smaller than 0.125. This means that the measurements of the bubble rise velocity in the column with the largest diameter (0.63 m) can be expected to be free of wall effects for the whole range of bubble sizes measured. As seen in Fig. 2, for the 0.63 m diameter column the measured rise velocities agree very well with the Mendelson equation [4]:

$$V_b = \sqrt{2\sigma / \rho_L d_b + g d_b / 2} \qquad (1)$$

The measured rise velocities in the smaller diameter columns were found to be significantly lower than that predicted by eq. (1), indicative of the strong wall effects.

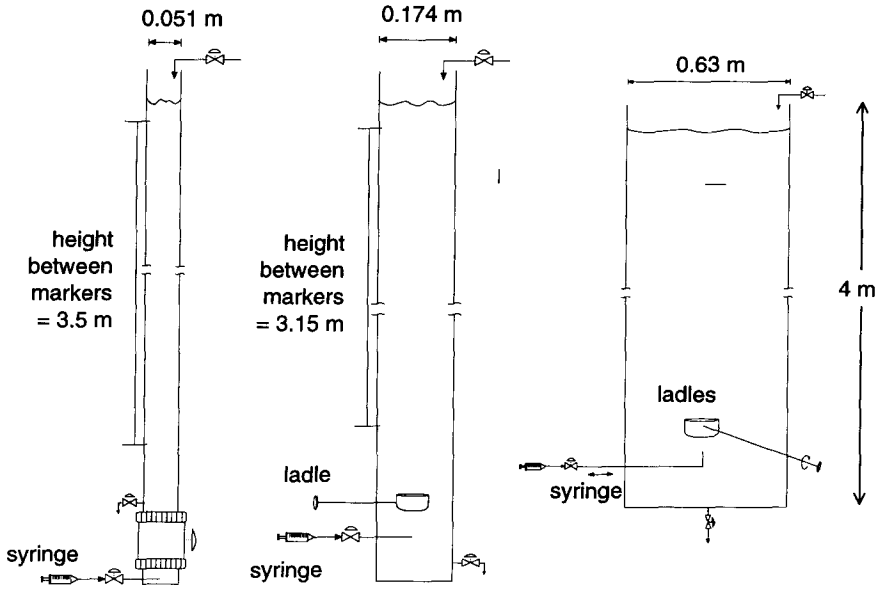

FIG. 1
Typical experimental set-ups for studies on rise velocity of single bubbles.

TABLE 1
Experimental set-up details and operating conditions for gas-liquid single bubble experiments.

Column diameter / [m]	Total height / [m]	Distance between markers / [m]	System studied	Bubble diameter range /[mm]	Number of experiments
0.01	1	0.9	air-water	3 - 6	60
0.02	1	0.9	air-water	3 – 11	106
0.03	1	0.9	air-water	3 – 17	120
0.051	4	3.5	air-water	3 - 49	506
0.10	6	5	air-water	3 - 48	311
0.10	2	1	Air-Tellus oil	13-72	147
0.174	4	3.15	air-water	3 - 47	842
0.630	4	3	air-water	3 - 79	595
Total number of experiments					2687

In order to quantify these wall effects we first consider the regime in which the bubbles have the shape of a spherical cap; this regime is characterized as one for which the Eötvös number, Eö > 40 (see Clift et al. [1]). For the air-water system, the criterion Eö > 40 is met for bubbles larger than 17 mm in diameter. As can be seen from Fig. 3 (a), the rise velocity data in cylindrical columns for all bubbles larger than 17 mm diameter agree very well with the estimations of the Collins relations [5]:

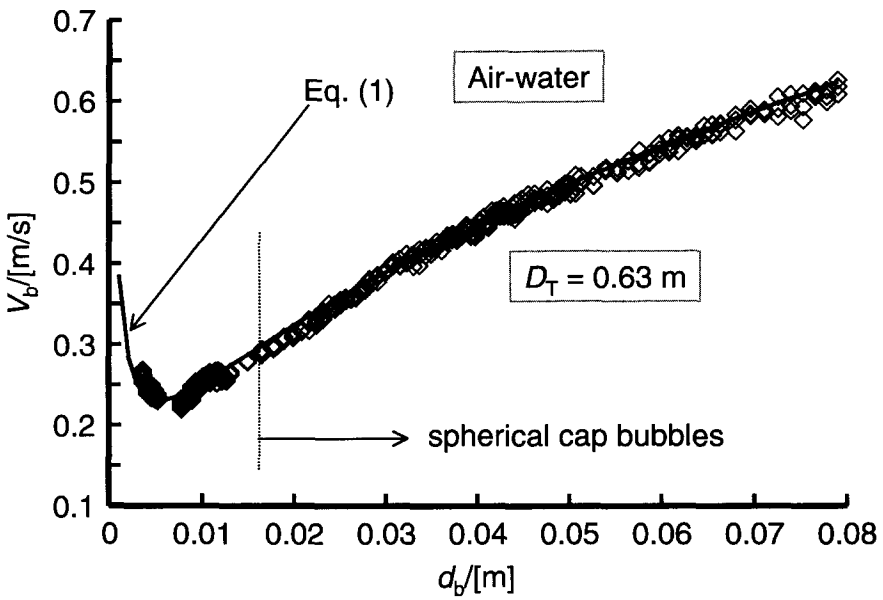

FIG. 2
Rise velocity of bubbles in a 0.63 m diameter column; comparison of experimental data with the predictions of the Mendelson equation [4]

$$V_b = \sqrt{g d_b/2}\, SF$$

$$SF = 1 \qquad \text{for } \frac{d_b}{D_T} < 0.125$$

$$SF = 1.13\exp\left(-\frac{d_b}{D_T}\right) \qquad \text{for } 0.125 < \frac{d_b}{D_T} < 0.6 \tag{2}$$

$$SF = 0.496\sqrt{D_T/d_b} \qquad \text{for } \frac{d_b}{D_T} > 0.6$$

The scale factor, *SF*, corrects the Davies-Taylor relation [6] for the influence of the wall on the single bubble rise velocity. For the air-Tellus oil system, the criterion Eö > 40 is met for bubbles larger than 13 mm in diameter and for this case also the Collins relations (2) describe the data accurately; see Fig. 3 (b). Equation (2) also applies for bubble rise in gas-solid fluidized beds [1].

The strong influence of the column diameter on the bubble rise velocity portrayed in eq. (2) is demonstrated by the retraced video recordings of the rise of a 34 mm diameter bubble in the 0.051 and 0.1 m diameter columns; see Fig. 4. It is to be noted that the bubble appears to be flatter in the 0.1 m diameter column.

For the bubble sizes in the range 3 – 17 mm, the deviation of the measured rise velocity to that predicted by eq. (1) is considered to be due to wall effects. From the experimental data we found that

$$V_b = \sqrt{2\sigma / \rho_L d_b + g d_b / 2}\, SF; \quad SF = \left[1 - (d_b / D_T)^2\right]^{3/2} \tag{3}$$

is a reasonable correlation of the data; see Fig. 5. The scale factor relation given in eq. (3) is the one suggested by Clift et al. [1].

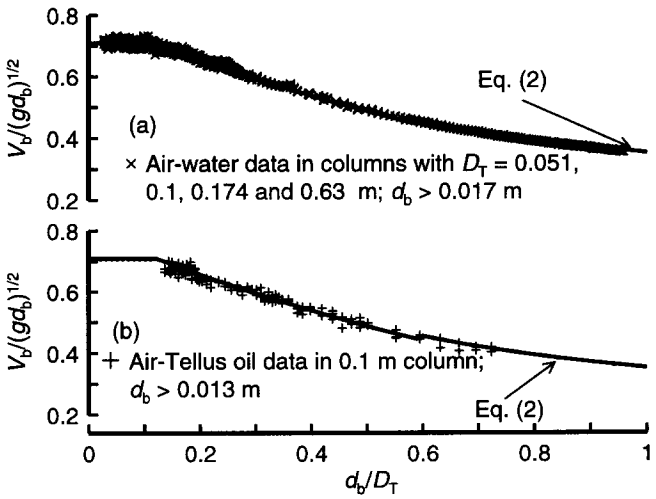

FIG. 3
Scale effects for rise of single gas bubbles in cylindrical columns. (a) Comparison of data for (a) air-water and (b) air-Tellus oil systems with the Davies-Taylor-Collins model.

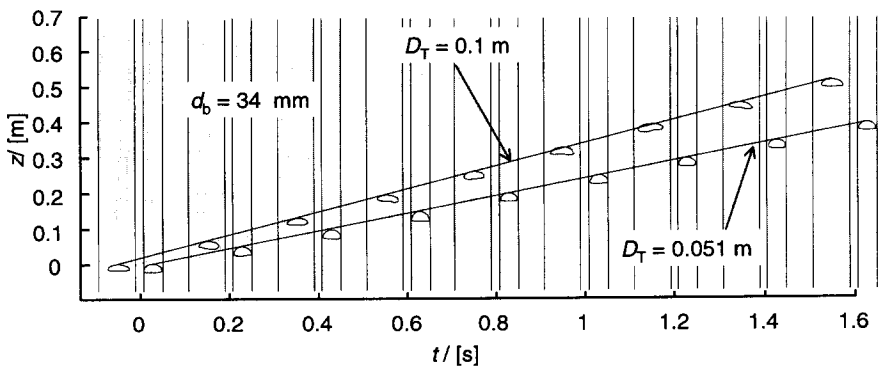

FIG. 4
Comparison of the rise trajectories of a 34 mm diameter bubble rising in water in columns of 0.051 and 0.1 m diameter. Experimentally obtained video images have been retraced.

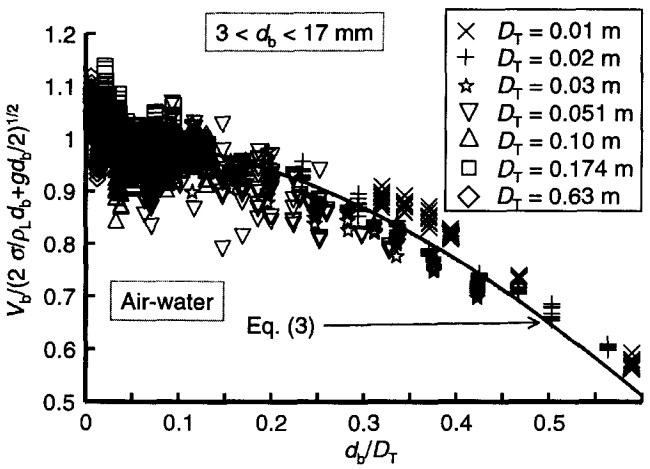

FIG. 5
Test of the modified Mendelson equation (3) with experimental data for the bubble size range of 3 – 17 mm.

Explanation of the Wall Effects

In order to understand the physics behind the wall effects on the rise velocity of single gas bubbles we performed some Volume-of-Fluid (VOF) simulations of the rise or air-bubbles in water. The VOF model [7,8,9,10] resolves the transient motion of the gas and liquid phases using the Navier-Stokes equations, and accounts for the topology changes of the gas-liquid interface induced by the relative motion between the dispersed gas bubble and the surrounding liquid. The finite-difference VOF model uses a donor-acceptor algorithm, originally developed by Hirt and Nichols [8], to obtain, and maintain, an accurate and sharp representation of the gas-liquid interface. The VOF method defines a fractional volume or "colour" function $c(\mathbf{x},t)$ that indicates the fraction of the computational cell filled with liquid. The colour function varies between 0, if the cell is completely occupied by gas, and 1, if the cell consists only of the liquid phase. The location of the bubble interface is tracked in time by solving a balance equation for this function:

$$\frac{\partial c(\mathbf{x},t)}{\partial t} + \nabla \bullet (\mathbf{u}c(x,t)) = 0 \qquad (4)$$

The liquid and gas velocities are assumed to equilibrate over a very small distance and essentially $\mathbf{u}_k = \mathbf{u}$ for k = L, G at the bubble interface. The mass and momentum conservation equations can be considered to be homogenous:

$$\nabla \bullet (\rho \mathbf{u}) = 0 \qquad (5)$$

$$\frac{\partial \rho \mathbf{u}}{\partial t} + \nabla \bullet (\rho \mathbf{u}\mathbf{u}) = -\nabla p - \nabla \bullet \tau + \rho \mathbf{g} + \mathbf{F}_{sf} \tag{6}$$

where p is the pressure, τ is the viscous stress tensor, $\mathbf{g}$ is the gravitational force. The density and viscosity used in eqs (5) and (6) are calculated from

$$\rho = \varepsilon_L \rho_L + \varepsilon_G \rho_G; \quad \mu = \varepsilon_L \mu_L + \varepsilon_G \mu_G \tag{7}$$

where ε_k denotes the volume fraction of the phase k = L,G. The continuum surface force model, originally proposed by Brackbill et al. [11], is used to model the force due to surface tension acting on the gas-liquid interface. In this model the surface tension is modelled as a body force $\mathbf{F}_{sf}$, that is non-zero only at the bubble interface and is given by the gradient of the colour function

$$\mathbf{F}_{sf} = \sigma \, \kappa(\mathbf{x}) \, \nabla c(\mathbf{x}, t) \tag{8}$$

where $\kappa(\mathbf{x})$ is the local mean curvature of the bubble interface:

$$\kappa(\mathbf{x}, t) = -\nabla \bullet \left(\mathbf{n} / |\mathbf{n}| \right) \tag{9}$$

where $\mathbf{n}$ is the vector normal to the bubble interface

$$\mathbf{n} = \nabla c(\mathbf{x}, t) \tag{10}$$

The set of equations (4) – (10) were solved using the commercial flow solver CFX 4.1c of AEA Technology, Harwell, UK. This package is a finite volume solver, using body-fitted grids. The grids are non-staggered and all variables are evaluated at the cell centers. An improved version of the Rhie-Chow algorithm [12] is used to calculate the velocity at the cell faces. The pressure-velocity coupling is obtained using the SIMPLEC algorithm [13].

All simulations reported here were carried out using the parallel version of CFX 4.1c running on a Silicon Graphics Power Challenge machine with six R800 processors. The simulations were carried out using a uniform 2D cartesian coordinate grid. The front of the 2D rectangular grid is formed by the *xz*–plane. The front and rear faces of the column are modelled as symmetry planes. At the two walls, the no-slip boundary condition is imposed. The column is modelled as an open system, so the pressure in the gas space above the initial liquid column is equal to the ambient pressure (101.325 kPa). For the convective terms in the equations hybrid differencing was used. Upwind differencing was used for the time integration. The time step used in the simulations were usually 0.0004 s or smaller. To counteract excessive smearing of the liquid-gas interface by numerical diffusion, a surface sharpening routine was invoked. This routine identifies gas and liquid on the "wrong" side of the interface, and moves it back to the correct side, while conserving volume of the respective phases. In order to avoid "dissolution" of the bubble due to surface sharpening we found it necessary to ensure that each bubble area encompassed a few hundred cells. For simulation of the rise of spherical cap bubbles, typically found with sizes above 17 mm, a grid size of 1 mm was found to be adequately small; in this case the number of grid cells per bubble cross-section was in excess of 300. For all simulations reported here a bubble neither gained nor

lost more than about 10% area during its rise. Animations of the simulations carried out to study the scale effects in 2D rectangular geometry can be viewed our web site http://ct-cr4.chem.uva.nl/cartesian/.

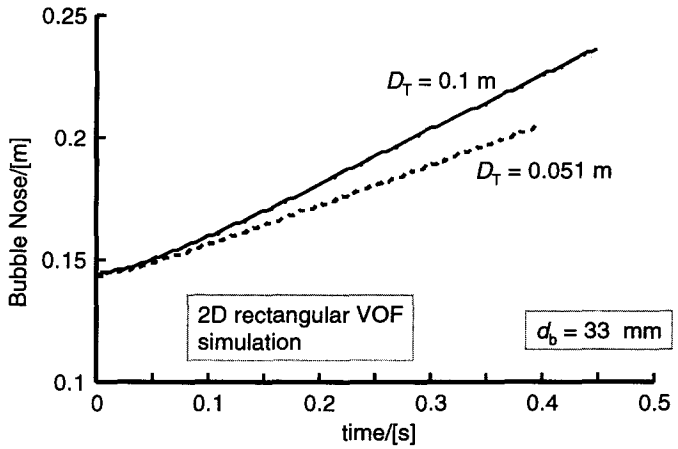

FIG. 6
The rise trajectories of 33 mm diameter bubbles in water determined from VOF simulations.

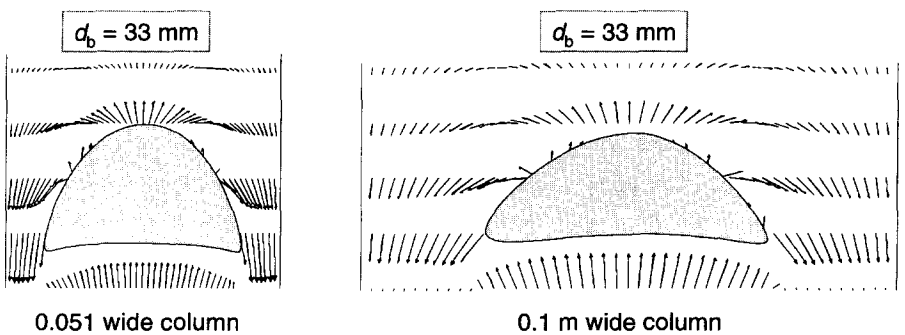

FIG. 7
Liquid phase velocity profiles surrounding a 33 m diameter bubble rising in columns of 0.051 and 0.1 m width.

Figure 6 compares the z-coordinates of the nose of 33 mm bubbles rising in columns of 0.1 and 0.051 m diameters; this figure shows that the bubble rises faster in the wider column. The reason for this is the restraining effect of the walls. Figure 7 shows the liquid phase velocity profiles for these two simulations. We notice that the 33 mm bubble assumes a flatter shape in the 0.1 m wide column and is less influenced by the wall than the same bubble placed in a 0.051 m wide column. This is in accordance with the video images obtained experimentally; see Fig. 4. Put another way, the drag between the bubble and the liquid is higher in the column of smaller width due to the higher downward liquid velocity in the vicinity of the bubble.

Concluding Remarks

1. The experimental data for bubble rise velocity of gas bubbles in the size range of 3 – 80 mm in columns of varying diameters, underlined the significant influence of column diameter on the rise velocity.
2. For spherical cap bubbles (meeting with the criterion Eö > 40) the Collins eq. (2) was found to be of excellent accuracy. This relation was validated on the basis of measurements with the air-water and air-Tellus oil systems.
3. The wall effect for spherical cap bubbles is found to be a unique function of the ratio of the bubble diameter to the column diameter, d_b/D_T. For $d_b/D_T > 0.6$, the bubble rise velocity is independent of the bubble diameter and is a function only of the column diameter; this can be seen from eq. (2). The maximum effect of the wall is to reduce the rise velocity by a factor of 0.496.
4. VOF simulations of the rise of single spherical cap bubbles show that the downward drag acting on the bubble is larger in a smaller diameter column.
5. For bubbles in the size range 3 – 17 mm, eq. (3) is recommended. This is the Mendelson [4] relation corrected for the column diameter influence.
6. The wall effect for bubbles in the 3 – 17 mm size range is shown in Figure 5 and we see that when $d_b/D_T = 0.6$, the effect is to reduce the rise velocity by factor of 2.

Nomenclature

$c(\mathbf{x},t)$	colour function, -
d_b	bubble diameter, m
D_T	column diameter, m
Eö	Eötvös number, $g(\rho_L - \rho_G)d_b^2/\sigma$
$\mathbf{F}_{sf}$	surface tension force, N m^{-3}
g	acceleration due to gravity, 9.81 m s^{-2}
$\mathbf{n}$	vector normal to the interface
r	radial coordinate, m
SF	scale factor, -
t	time, s
$\mathbf{u}$	velocity vector, m s^{-1}
V_b	rise velocity of the bubble, m s^{-1}

z	distance coordinate along height of cylindrical column, m
ε	volume fraction of phase, -
$\kappa(x)$	curvature of bubble interface, -
μ	viscosity of phase, Pa s
ρ	density of phases, kg m^{-3}
σ	surface tension, N m^{-1}
τ	viscous stress tensor, N m^{-2}

Subscripts

b	referring to bubble
G	referring to gas phase
L	referring to liquid phase
T	tower or column

References

1. R. Clift, J.R. Grace and M.E. Weber, Bubbles, drops and particles. Academic Press, San Diego (1978).
2. L.S. Fan and K. Tsuchiya, Bubble wake dynamics in liquids and liquid-solid suspensions, Butterworth Heinemann, Boston (1990).
3. G.B. Wallis, One-dimensional two-phase flow. McGraw-Hill, New York (1969).
4. H.D. Mendelson, *A.I.Ch.E.J.*, **13**, 250 (1967).
5. R. Collins, *J. Fluid Mech.*, **28**, 97 (1967).
6. R.M.Davies and G.I. Taylor, *Proc. Roy. Soc. London* **A200**, 375 (1950).
7. E. Delnoij, J.A.M.Kuipers and W.P.M. van Swaaij, *Chem. Eng. Sci.*, **52**, 3623 (1997).
8. C.W. Hirt and B.D. Nichols, *J. Computational Physics*, **39**, 201 (1981).
9. A. Tomiyama, I. Zun, A. Sou and T. Sakaguchi, *Nuclear Engineering and Design*, **141**, 69 (1993).
10. A. Tomiyama, A. Sou, H. Minagawa and T. Sakaguchi, *JSME International Journal, Series B*, **36**, 51(1993).
11. J.U. Brackbill, D.B. Kothe and C. Zemarch, *J. Comput. Physics*, **100**, 335 (1992).
12. C.M. Rhie and W.L. Chow, *AIAA Journal*, **21**, 1525 (1983).
13. J. Van Doormal, and G.D. Raithby, *Numer. Heat Transfer*, **7**, 147 (1984).

Received February 8, 1999